Received: 9 December 2022 | Revised: 2 February 2023 | Accepted: 28 February 2023

DOI: 10.1002/cyto.a.24728

ORIGINAL ARTICLE

MIFlowCyt

ISAC CYTOMETRY Journal of Quantitative Cell Science PART A

Improved estimation of the ratio of detection efficiencies of excited acceptors and donors for FRET measurements

Ágnes Batta[1,2] | Tímea Hajdu[1] | Peter Nagy[1]

[1]Faculty of Medicine, Department of Biophysics and Cell Biology, University of Debrecen, Debrecen, Hungary

[2]Faculty of Medicine, Doctoral School of Molecular Medicine, University of Debrecen, Debrecen, Hungary

Correspondence
Peter Nagy, Faculty of Medicine, Department of Biophysics and Cell Biology, University of Debrecen, Debrecen, Hungary.
Email: nagyp@med.unideb.hu

Funding information
National Research, Development and Innovation Office, Hungary, Grant/Award Numbers: K138075, ANN133421; Faculty of Medicine, University of Debrecen

Abstract

Förster resonance energy transfer (FRET) is a radiationless interaction between a donor and an acceptor whose distance dependence makes it a sensitive tool for studying the oligomerization and the structure of proteins. When FRET is determined by measuring the sensitized emission of the acceptor, a parameter characterizing the ratio of detection efficiencies of an excited acceptor versus an excited donor is invariably involved in the formalism. For FRET measurements involving fluorescent antibodies or other external labels, this parameter, designated by α, is usually determined by comparing the intensity of a known number of donors and acceptors in two independent samples leading to a large statistical variability if the sample size is small. Here, we present a method that improves precision by applying microbeads with a calibrated number of antibody binding sites and a donor-acceptor mixture in which donors and acceptors are present in a certain, experimentally determined ratio. A formalism is developed for determining α and the superior reproducibility of the proposed method compared to the conventional approach is demonstrated. Since the novel methodology does not require sophisticated calibration samples or special instrumentation, it can be widely applied for the quantification of FRET experiments in biological research.

KEYWORDS
FRET, calibration, fluorescence microscopy

1 | INTRODUCTION

Förster resonance energy transfer (FRET) is a radiationless interaction between a donor and an acceptor whose efficiency is a function of the sixth power of the donor-acceptor distance. It is this property of FRET that makes it sensitive to clustering and conformation laying the foundations for its widespread application in biology and even in the medical laboratory [1–3]. Although FRET was first observed by the Perrins in the 1920s [4] and adequately described by Förster just after World War II [5], its biological application required the availability of instruments to measure it in samples of biological interest, and methods for labeling biologically relevant molecules with fluorescent tags. For these reasons, FRET finally came of age in the 1980s and it has been enjoying widespread popularity ever since due to its capability to provide information on the nanometer scale, a remarkable achievement even in the era of superresolution [6].

Although FRET is manifested in a number of measurable changes in the properties of the donor and the acceptor [7], the easiest and most popular approach for its measurement involves detection of FRET-sensitized acceptor emission, that is, excitation of the donor

and subsequent recording of fluorescence of the acceptor. Despite the principal simplicity of such ratiometric or intensity-based measurements, quantitative determination of the FRET efficiency requires a complex equation set, whose frightening nature led to the introduction of various FRET-related parameters whose linearity with respect to the FRET efficiency and the extent of oligomerization has been questioned [8, 9]. Therefore, calculation of the FRET efficiency is preferred whose experimental determination obviously varies, but it usually involves measurement of three fluorescence intensities in the donor, FRET and acceptor channels [6, 8]. Although the formalism has not substantially changed since its development in the 1980s [10], fluorophore saturation, a common confounding factor in confocal microscopy, has been shown to introduce systematic distortions into the calculations [11]. Since each of the measured intensities is contaminated by overspilled intensities of other detection channels, several spectral compensation parameters have to be introduced into the equation set. Since FRET is manifested in the disappearance of an excited donor and the generation of an excited acceptor, intensity-based FRET approaches invariably involve a parameter comparing the detection efficiencies of these two molecular species. This variable is going to be labeled by α in accordance with previous publications [10–14], although G and γ have also been used for its designation [15]. Since the detection efficiency of an excited fluorophore is determined by the fluorophore's fluorescence quantum yield and the detection efficiency of its emitted photons, α is defined according to the following equation:

$$\alpha = \frac{Q_A \eta_{A2}}{Q_D \eta_{D1}} \quad (1)$$

where Q_A and Q_D refer to the quantum yield of the acceptor and the donor, respectively, and η_{A2} and η_{D1} are the detection efficiencies of the acceptor photons in the FRET channel and that of the donor photons in the donor channel, respectively. However simple this equation is, it proved hard to tackle experimentally. While determination of the quantum yield is relatively simple [16, 17], the detection efficiency is notoriously complicated to measure. Therefore, almost all of the reported experimental approaches for determining α revolve around the principle of comparing the intensity of a known number of donors and acceptors. Many different realizations of this principle have been developed for fluorescent proteins since it is relatively easy to generate FRET constructs in which the donor and acceptor fluorescent proteins are expressed as a single protein connected by a linker. It was a regression approach requiring an arbitrary number of such constructs that pioneered these methods [18] followed by a similar approach based on two such FRET constructs [19]. The same principle is used in single-molecule FRET measurements in which the different FRET constructs are replaced by different conformations of the same FRET probe [20]. In two consecutive publications, an iterative and a closed-form approach have been developed for determining α for a single donor-acceptor fluorescent protein construct [21, 22]. The increasing availability of FRET constructs with known energy transfer efficiencies prompted the development of an "inverse" approach in which α is adjusted so that the FRET efficiency calculated for a particular FRET probe equals its known energy transfer efficiency [23].

The number and scope of methods for determining α for FRET studies with external fluorescent labels, such as antibodies, Fabs, single-chain antibodies, darpins, and so forth, is more limited. The first such approach was described in the paper in which flow cytometric energy transfer was introduced, and it is based on directly comparing the intensities of two samples labeled either by the donor only or by the acceptor only. After correcting for the molar absorption coefficients of the dyes and the degree of labeling of the labels, α can be determined [10]. Recently, the formula has been modified to account for fluorophore saturation [11]. The accuracy of the method is undermined by the fact that the degree of labeling of the stock solution and the bound fraction are assumed to be equal, which was reported to be not the case [24]. Precision of the method hinges upon the assumption that the two compared samples contain an equal number of donors and acceptors, a requirement that is only met if large number of cells are measured. Consequently, reproducibility of the approach may deteriorate significantly in microscopy. A different methodology has been put forward in which the extent to which the donor intensity is dequenched is compared to the loss in acceptor intensity during partial acceptor photobleaching of the FRET sample [25]. A limitation of this approach is that it can only be applied if spillover of the directly excited acceptor intensity to the FRET channel is negligible. Two rather complex methods have been published that are based on entirely different principles, but they have only been tested in flow cytometry [26, 27]. Since the major drawback of comparing the donor and acceptor intensities in two samples is the statistical uncertainty if a low number of cells are measured, the principle could be adapted to microscopy by labeling cells with antibodies binding to noncompeting epitopes in the same protein between which no energy transfer takes place [14]. Here, we propose a novel, more generally applicable method in which statistical variability of this principle is reduced by applying microspheres with a calibrated number of antibody binding sites and by labeling such beads or cells with a mixture of donor- and acceptor-conjugated antibodies. The fact that the method has been implemented in Excel and its simplicity suggest that it can be widely used for calibration of intensity-based FRET measurements with external labels.

2 | MATERIALS AND METHODS

2.1 | Cells, antibodies and microspheres

The SKBR-3 and A431 cell lines were obtained from the American Type Culture Collection (ATCC; Manassas, VA), and they were cultured according to their specifications. Trastuzumab, a humanized monoclonal antibody against ErbB2, was purchased from Roche-Hungary (Budapest, Hungary). Cetuximab, a humanized monoclonal antibody against epidermal growth factor receptor (EGFR), was obtained from Merck-Hungary (Budapest, Hungary). The Mab528 monoclonal antibody against EGFR was purified from the supernatant

of the HB-8509 mouse hybridoma cell line (ATCC) by protein A affinity chromatography. Succinimidyl ester derivatives of AlexaFluor488 and AlexaFluor546 (Thermo Fisher Scientific, Waltman, MA) were conjugated to purified monoclonal antibodies according to the manufacturer's specifications. The degree of labeling of the fluorescent antibodies was determined by spectrophotometry. Quantum Simply Cellular (QSC) beads with calibrated antibody binding capacity, coated with anti-human or anti-mouse Fc-specific antibodies, were purchased from Bangs Laboratories (Fishers, IN).

Cultured cells were trypsinized, washed in PBS and $5{\cdot}10^5$ cells were resuspended in 50 µL PBS supplemented with 0.5 mg/mL BSA for labeling with fluorescent antibodies at a concentration of 20 µg/mL for 30 min on ice. For labeling QSC microspheres, two drops of the bead suspension was placed in a tube, and the same labeling protocol was applied. One drop of the bead suspension contains ~100,000 beads, and it corresponds to ~50 µL according to our own determination and the company's specification. After labeling, unbound antibodies were removed by centrifugation, and the cells were fixed in 1% formaldehyde before subsequent measurements by flow cytometry or confocal microscopy.

2.2 | Flow cytometry

Samples were measured in a NovoCyte® 3000 RYB flow cytometer (ACEA Biosciences, Inc. San Diego, CA). AlexaFluor488 (Thermo Fisher Scientific) was excited with the 488-nm laser and was detected at 530/30 nm; AlexaFluor546 (Thermo Fisher Scientific) was excited with the 561-nm laser line and detected at 586/20 nm. For detecting FRET-sensitized emission of AlexaFluor546 (FRET channel), the samples were excited with the 488-nm laser line and detected at 586/20 nm. Flow cytometric data were analyzed in FCS Express 6 Flow Research Edition (De Novo, Pasadena, CA). Live cells or singular beads were gated on the forward scatter–side scatter dot plot followed by determining the mean fluorescence intensity of the gated subpopulation.

2.3 | Confocal microscopy and image analysis

Trypsinized samples identical to those used for flow cytometry were measured by confocal microscopy. The samples were transferred to a µ-slide 8-well Ibidi chamber (Gräfelfing, Germany) after centrifugation. Images were recorded with a Zeiss LSM880-Airy-scan confocal laser scanning microscope (Carl Zeiss AG, Oberkochen, Germany) using a water immersion, C-Apochromat 40× (NA = 1.2) objective. The fluorescence of AlexaFluor488 was excited at 488 nm and detected in the spectral range 493–557 nm (donor channel, I_1). AlexaFluor546 was excited at 543 nm, and its emission was recorded between 560 and 670 nm (acceptor channel, I_3). Sensitized emission (FRET channel, I_2) was monitored by exciting the samples at 488 nm and recording their fluorescence between 560 and 670 nm. Images were analyzed in Matlab (Mathworks, Natick, MA) using the DipImage toolbox (Delft University of Technology, Delft, The Netherlands). The cell membrane or the edge of microspheres was identified using a custom-written implementation of the manually-seeded watershed segmentation algorithm on gray-scale images smoothed by a Gaussian kernel. Mean intensities of individual cells or microbeads were calculated in pixels corresponding to the mask determined by watershed segmentation. These individual intensities were saved in a Matlab variable for further statistical analysis (for details see the "Statistical analysis" section).

2.4 | Calculation of the FRET efficiency

The FRET efficiency from confocal microscopic images was calculated using a custom-written program, rFRET, in Matlab [28]. The program solves the equation set to be described in detail in the theory section (Equation (3)). Images were first segmented by the manually-seeded watershed segmentation algorithm, and calculations were only performed with pixels corresponding to the cell membrane or edge of microbeads. We opted for using the mean intensities determined in the whole mask for the FRET calculations to make these calculations principally similar to those used for determining parameter α. While using mean intensities is essential due to the assumption of an equal number of fluorophores (conventional approach) or a known ratio of donor and acceptors (R'-based method) in calculation of α, it would have been possible to do the FRET determination on a pixel-by-pixel basis. In an intensity-based FRET experiment, fluorescence is measured in the donor (I_1), FRET (I_2) and acceptor (I_3) channels. Fluorescence in the donor and FRET channels is excited at the donor excitation wavelength, while the acceptor excitation wavelength is used for the acceptor channel. Emission is measured in the spectral range of the donor in the donor channel, while the acceptor emission range is used for the FRET and acceptor channels. Overspill parameters of the donor were determined using samples labeled by the donor only, while the acceptor overspill parameters were calculated in acceptor-only labeled cells. These overspill factors and parameter α were used for determining the FRET efficiency.

2.5 | Conventional determination of parameter α using two different samples (conventional approach)

Since parameter α describes the ratio of fluorescence intensities of an equal number of excited acceptors and donors, its experimental determination usually involves the comparison of mean intensities of samples to which an equal number of donor-tagged and acceptor-tagged antibodies are bound according to the following Equation (10):

$$\alpha = \frac{\overline{I_{2,A}}}{\overline{I_{1,D}}} \frac{L_D \varepsilon_D{}^D}{L_A \varepsilon_A{}^D} \tag{2}$$

where $\overline{I_{2,A}}$ is the mean intensity of a sample labeled by an acceptor-conjugated antibody measured in the FRET channel, and $\overline{I_{1,D}}$ is the

mean donor intensity of another sample that is labeled by the donor-conjugated version of the same antibody. The $\overline{I_{2,A}}/\overline{I_{1,D}}$ ratio describes the intensity ratio of two samples labeled by the same number of antibodies, and not by the same number of fluorophores. Multiplying it with L_D/L_A, where L_D and L_A are the degrees of labeling of the donor-conjugated and acceptor-conjugated antibodies, respectively, provides a parameter corresponding to the ratio of intensities of the same number of acceptor and donor dyes. Since α is the intensity ratio of the same number of excited acceptors and donors, the equation must also contain a correction for their different excitability characterized by their molar absorption coefficients ($\varepsilon_D{}^D$ – molar absorption coefficient of the donor at the excitation wavelength of the donor; $\varepsilon_A{}^D$ – molar absorption coefficient of the acceptor at the excitation wavelength of the donor).

In order to determine α, a sample was labeled with donor-tagged antibodies and its intensity was recorded in the donor channel. This image was segmented using manually-seeded watershed segmentation, and intensities in the foreground were determined ($\overline{I_{1,D}}$). Another sample, labeled with the acceptor-conjugated version of the same antibody, was imaged in the FRET and acceptor channels. Images recorded in the acceptor channel were used for watershed-based identification of edge pixels, and the mean intensity recorded in the FRET channel was determined in them ($\overline{I_{2,A}}$). The mean intensities along with the degrees of labeling and the molar absorption coefficients were substituted into Equation (2) for calculating α. Principles of the image analysis procedure are demonstrated by Supplementary Figure S1.

2.6 | Statistical analysis

In order to estimate the standard error of the mean as a function of sample size, a resampling approach was taken. The fluorescence intensity of each individual cell or microsphere in a single kind of measurement (~200 cells) was determined and saved in a Matlab variable. For calculating α according to the conventional approach (Equation (2)), 100 samples of different sizes ranging between 1 and 100 were taken with replacement from the database containing intensities of donor-only and acceptor-only cells. The procedure, also known as bootstrapping, allows every bead or cell to be sampled repeatedly, and it mimicks the sampling process during a measurement. α was calculated according to Equation (2) using the mean intensities of the virtual samples followed by determining the standard error of the mean of all α values for a given sample size. When estimating the precision of the determination of α according to the proposed method involving antibody mixtures, 100 cells or microspheres were randomly chosen with replacement from the database of double-labeled cells/beads, and α was calculated according to Equation (15) using the mean donor (I_1), FRET (I_2) and acceptor (I_3) intensities followed by determining the standard error of the mean of all α values for a given sample size. The principle of the resampling approach is demonstrated in Supplementary Figure S2.

3 | THEORY

For determining the FRET efficiency, the intensities measured in the donor (I_1), FRET (I_2) and acceptor channels (I_3) of a donor-acceptor double-labeled sample are described by the following equation set:

$$\begin{aligned} I_1 &= I_D(1-E) + I_A S_4 + I_D E \alpha \frac{S_4}{S_2} \\ I_2 &= I_D(1-E) S_1 + I_A S_2 + I_D E \alpha \\ I_3 &= I_D(1-E) S_3 + I_A + I_D E \alpha \frac{\varepsilon_2}{S_2} \end{aligned} \tag{3}$$

where S_1 and S_3 are parameters characterizing the overspill of the donor to the FRET and acceptor channels, respectively, while S_2 and S_4 describe the overspill of the acceptor to the FRET and donor channels, respectively. I_D, I_A and E are the unquenched donor intensity, the directly-excited acceptor intensity and the FRET efficiency, respectively, and ε_2 is the ratio of molar absorption coefficients according to the following equation:

$$\varepsilon_2 = \frac{\varepsilon_D{}^A \, \varepsilon_A{}^D}{\varepsilon_D{}^D \, \varepsilon_A{}^A} \tag{4}$$

where subscripts D and A refer to the fluorophore type (D – donor, A – acceptor), and superscripts refer to the wavelength at which the molar absorption coefficient is determined (D – donor excitation wavelength, A – acceptor excitation wavelength). Since this set of three equations contains three unknowns, it can be solved. If α is to be determined from this same equation set, it will be the fourth unknown, and the system can only be solved if another independent equation is added to the set.

3.1 | Derivation of a relationship between I_D and I_A

If the donor-acceptor ratio is one, a relationship between I_D and I_A is easy to formulate [14, 22]. Let us introduce this fourth equation into the equation set for the general case when the numbers of donors and acceptors are not equal. It is possible to relate the donor and acceptor intensities (I_D and I_A) to each other if cells or beads are labeled with a mixture of donor-tagged and acceptor-tagged antibodies that compete for the same binding sites. This situation arises if antibodies against the same epitope are mixed for labeling cells, or when beads with Fc-binding sites are labeled with a mixture of two different antibody types. Let us designate the fraction of epitopes occupied by donor-tagged antibodies by R:

$$R = \frac{N_D}{N_0} \tag{5}$$

where N_D and N_0 are the number of bindings sites occupied by the donor-labeled antibody and the total number of binding sites, respectively. Assuming that the binding sites are saturated, that is,

$N_D + N_A = N_0$ (N_A – number of binding sites occupied by acceptor-conjugated antibodies), the N_A/N_D ratio is expressed by the following equation:

$$\frac{N_A}{N_D} = \frac{1-R}{R} \tag{6}$$

Let us express the donor intensity (I_D) and the acceptor intensity (I_A) by the following equations:

$$\begin{aligned} I_D &= N_D L_D \Phi_D \varepsilon_D{}^D Q_D \eta_{D1} \\ I_A &= N_A L_A \Phi_A \varepsilon_A{}^A Q_A \eta_{A3} \end{aligned} \tag{7}$$

where L_D and L_A are the degrees of labeling of the donor-conjugated and acceptor-conjugated antibodies, respectively, Φ_D and Φ_A are the photon densities of the laser exciting the donor and the acceptor, respectively, Q_D and Q_A are the fluorescence quantum efficiencies of the donor and the acceptor, respectively, and η_{D1} and η_{A3} are the detection efficiencies of donor photons in the donor channel and that of acceptor photons in the acceptor channel, respectively. According to Equation (7), the fluorescence intensity is linearly proportional to the excitation intensity (photon density). This relationship only holds if fluorophores are not saturated [11]. Since fluorophore saturation undermines many assumptions of quantitative microscopy, it is strongly advisable to establish that fluorophores are not saturated, for example, by observing a linear dependence of fluorescence intensity on excitation power. Dividing I_A by I_D and by replacing the N_A/N_D ratio with Equation (6) yields the following result:

$$\frac{I_A}{I_D} = \frac{L_A(1-R)\,\Phi_A \varepsilon_A{}^A Q_A \eta_{A3}}{L_D R \Phi_D \varepsilon_D{}^D Q_D \eta_{D1}} \tag{8}$$

For the previous equation to be of practical value, difficult-to-measure parameters should be eliminated. S_2 can be defined according to the following equation [11, 29]:

$$S_2 = \frac{\Phi_D \varepsilon_A{}^D \eta_{A2}}{\Phi_A \varepsilon_A{}^A \eta_{A3}} \tag{9}$$

where η_{A2} and η_{A3} are the detection efficiencies of acceptor photons in the FRET and acceptor channels, respectively. Using this expression for S_2 and the definition of α (Equation (1)), Equation (8) can be rewritten:

$$\frac{I_A}{I_D} = \frac{L_A(1-R)\,\alpha}{L_D R S_2 \varepsilon_1} \tag{10}$$

where

$$\varepsilon_1 = \frac{\varepsilon_D{}^D}{\varepsilon_A{}^D} \tag{11}$$

Since the intensity ratio I_A/I_D is determined by both R and the degrees of labeling of the antibodies, let us define a new variable, R' incorporating both terms:

$$R' = \frac{L_A(1-R)}{L_D R} \tag{12}$$

Using R', the intensity ratio I_A/I_D can be expressed according to the following equation:

$$\frac{I_A}{I_D} = \frac{R'\,\alpha}{S_2\,\varepsilon_1} \tag{13}$$

3.2 | Determination of R'

Let us supplement equation set [3] of a donor-acceptor double-labeled sample with the equation relating the donor and acceptor intensities (Equation (13)) and solve it for R':

$$R' = \frac{S_2\,\varepsilon_1\left(-\varepsilon_2\overline{I_2} + \varepsilon_2\overline{I_1}\,S_1 + \overline{I_3}\,S_2 - \overline{I_1}\,S_2\,S_3 - \overline{I_3}\,S_1\,S_4 + \overline{I_2}\,S_3\,S_4\right)}{\overline{I_2}\left(S_2 - S_2\,S_3\,S_4 + (\varepsilon_2 - 1)S_4\,\alpha\right) + S_2\left(-\overline{I_3}\,S_2 + \overline{I_3}\,S_1\,S_4 + \overline{I_1}(-S_1 + S_2\,S_3 + \alpha - \varepsilon_2\,\alpha)\right)} \tag{14}$$

In this equation, $\overline{I_1}$, $\overline{I_2}$ and $\overline{I_3}$ correspond to the mean intensities measured in the donor, FRET and acceptor channels, respectively, and not to cell-by-cell intensities. This equation is used for determining parameter R' of an antibody mixture using a device providing statistically robust results (e.g., flow cytometry). Once R' of a certain mixture has been determined, this R' value can be used to determine α of the same antibody mixture in microscopy (see next section). Reliability of this approach hinges upon the statistical robustness of α in Equation (14), which is the α parameter of the flow cytometer determined according to Equation (2). The fact that flow cytometry measures a large number of cells ensures that α can be assumed to be unaffected by statistical variability stemming from the low number of measured cells. Therefore, the R' parameter will be statistically reliable as well. The Excel file "alpha from R and QSC.xlsm" available as supplementary material calculates R' according to Equation (14).

3.3 | Determination of α in microscopy

Once R' has been determined by flow cytometry, it will be used to calculate α using a cell or QSC bead sample labeled with the same mixture of donor-tagged and acceptor-tagged antibodies whose R' value is already known. The same equations, that is, equation set [3] supplemented with Equation (13), will be used to this end as well, but R' is a known parameter now, and therefore the equation set can be solved for α, E, I_D and I_A:

$$\alpha = \frac{S_2\left(-\overline{I_3}(S_2 - S_1 S_4)(R' + \varepsilon_1) + \overline{I_1}(-R' S_1 + R' S_2 S_3 - \varepsilon_1 \varepsilon_2 S_1 + \varepsilon_1 S_2 S_3) + \overline{I_2}(R' - R' S_3 S_4 + \varepsilon_1(\varepsilon_2 - S_3 S_4))\right)}{(\varepsilon_2 - 1)R'\left(\overline{I_1} S_2 - \overline{I_2} S_4\right)}$$

$$E = \frac{R'\left(\overline{I_1}(S_1 - S_2 S_3) + \overline{I_3}(S_2 - S_1 S_4) + \overline{I_2}(S_3 S_4 - 1)\right)}{\varepsilon_1\left(\varepsilon_2\left(\overline{I_2} - \overline{I_1} S_1\right) - \overline{I_3} S_2 + \overline{I_1} S_2 S_3 + \overline{I_3} S_1 S_4 - \overline{I_2} S_3 S_4\right)}$$

$$I_D = \frac{\varepsilon_1\left(\overline{I_1} S_2 - \overline{I_2} S_4\right)\left(\varepsilon_2\left(\overline{I_2} - \overline{I_1} S_1\right) - \overline{I_3} S_2 + \overline{I_1} S_2 S_3 + \overline{I_3} S_1 S_4 - \overline{I_2} S_3 S_4\right)}{(S_2 - S_1 S_4)\left(-\overline{I_3}(S_2 - S_1 S_4)(R' + \varepsilon_1) + \overline{I_1}(-R' S_1 + R' S_2 S_3 - \varepsilon_1 \varepsilon_2 S_1 + \varepsilon_1 S_2 S_3) + \overline{I_2}(R' - R' S_3 S_4 + (\varepsilon_2 - S_3 S_4)\varepsilon_1)\right)}$$

$$I_A = \frac{\varepsilon_2\left(\overline{I_2} - \overline{I_1} S_1\right) - \overline{I_3} S_2 + \overline{I_1} S_2 S_3 + \overline{I_3} S_1 S_4 - \overline{I_2} S_3 S_4}{(\varepsilon_2 - 1)(S_2 - S_1 S_4)} \tag{15}$$

TABLE 1 Antibodies used in the experiments.

	Anti-ErbB1 (Mab528)		Anti-ErbB2 (trastuzumab)	
	AlexaFluor488	AlexaFluor546	AlexaFluor488	AlexaFluor546
Low DOL	DOL = 0.91	DOL = 0.98	DOL = 1.38	DOL = 1.12
High DOL	DOL = 4.55	DOL = 4.85	DOL = 4.41	DOL = 3.4

Note: The antibodies binding to ErbB1 and ErbB2 were Mab528 and trastuzumab, respectively. They were conjugated with AlexaFluor488 or AlexaFluor546 in low and high dye-to-protein ratios. The degree of labeling (DOL) of the antibodies used in the FRET experiments are shown in the table.

Just as in the case of Equation (14), the intensities ($\overline{I_1}$, $\overline{I_2}$ and $\overline{I_3}$) are mean intensities, and not pixelwise intensities. These equations only contain the intensities of a single sample, the donor-acceptor double-labeled one. Since the error of mean intensities scales inversely with the square root of the sample size, means determined from few events are inherently unreliable. Error in mean calculations originates from measurement errors (photon statistics) and the biological variability of the samples. If the mean of a ratio of intensities of two different samples, for example, Equation (2), is to be calculated, the error of the mean will be increased due to the fact that two different samples are compared whose protein expression levels are not equal. If a function of intensities, for example, α, E, I_D and I_A in Equation (15), only contains the intensities of a single sample, this error source is eliminated. Therefore, parameter α calculated according to Equation (15) will have much less error than that calculated according to Equation (2) even if mean intensities are calculated from few cells. The Excel file "alpha from R and QSC.xlsm" available as supplementary material calculates α from the mean intensities and the required additional parameters. The workflow of the whole calculation is summarized in Supplementary Table 1.

4 | RESULTS

4.1 | Reducing the variance of parameter α by using microspheres with a calibrated number of antibody binding sites

Determination of α for FRET measurements between fluorescently-labeled antibodies according to Equation (2) hinges upon the assumption that the number of binding sites for the donor-labeled antibody in the donor-only sample is identical to the number of binding sites for the acceptor-labeled antibody in the acceptor-only sample. While this assumption is valid when a large number of cells are measured, it is the bottleneck of the calculation in microscopy when orders of magnitude fewer cells can be measured than in flow cytometry. We reasoned that microspheres with a calibrated number of antibody binding sites might improve the precision of α determination since the variability of the number of antibody binding sites is significantly lower than in cells. We tested protein A and protein G beads used for immunoprecipitation, but the intensity distribution after labeling them with fluorescent antibodies was too wide according to flow cytometry. Therefore, we turned to Quantum Simply Cellular (QSC) beads and used one of the three brightest subpopulations for the measurements. The characteristics of the antibodies are summarized in Table 1. A431 cells were labeled with AlexaFluor488-Mab528 (DOL = 0.91), and another sample of A431 cells was labeled with AlexaFluor546-Mab 528 (DOL = 0.98). The mean intensities of these samples were determined and α was calculated according to Equation (2). On a single day, four such pairs of samples were recorded, and the standard error of the mean of α was calculated. In order to determine α for an antibody pair with high degree of labeling, pairs of A431 cell samples were prepared using AlexaFluor488-Mab528 (DOL = 4.55) and AlexaFluor546-Mab528 (DOL = 4.85), and α and its error were determined as above. Alongside these cellular samples, QSC beads were also labeled with the same antibodies, and α and its error were determined as described above. α depends on the degree of labeling and also on whether it is determined using cells or QSC beads (Figure 1B). The standard error of the mean of α calculated with QSC beads was ⅓ – ½ of those

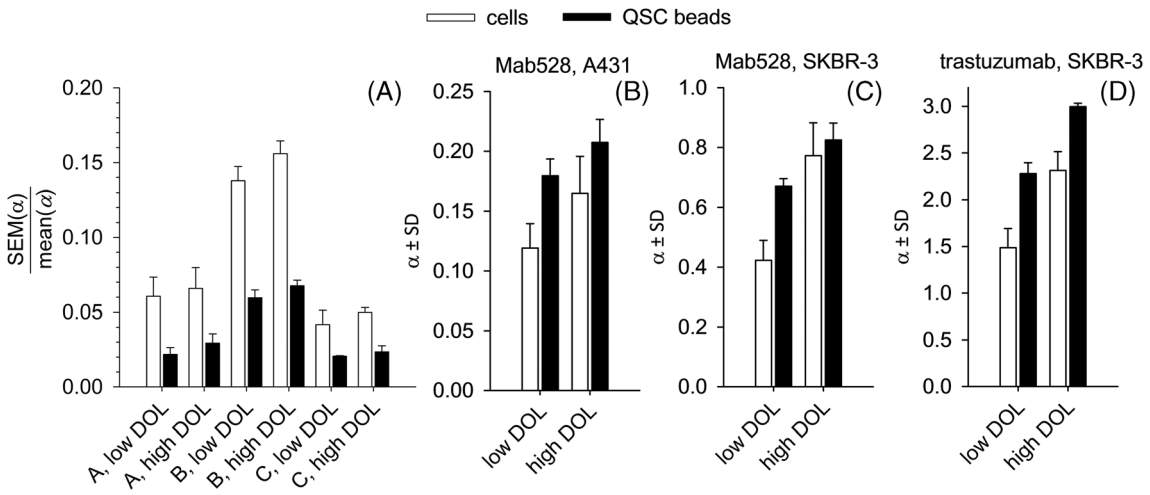

FIGURE 1 Determination of parameter α according to the conventional method using cells and QSC beads. A cell sample was labeled with donor-conjugated antibody, and another cell sample was labeled with the acceptor-conjugated version of the same antibody (B – AlexaFluor488-Mab528 + AlexaFluor546-Mab528 on A431 cells; C – AlexaFluor488-Mab528 + AlexaFluor546-Mab528 on SKBR-3 cells; D – AlexaFluor488-trastuzumab + AlexaFluor546-trastuzumab on SKBR-3 cells). The same strategy was followed when labeling QSC beads. Antibodies with low and high degree of labeling were used (see Table 1 for antibody characteristics). Parameter α was calculated according to the conventional approach using Equation (2). This method requires the mean intensity of the donor-labeled sample and the mean intensity of the sample labeled with the acceptor-conjugated version of the same antibody. Labels "low DOL" on the horizontal axes identify calculations in which the degree of labeling of both the donor- and acceptor-labeled antibodies was low, whereas for calculations labeled by "high DOL", both antibodies had a high degree of labeling. The standard error of the mean of five independent measurements was calculated and normalized by the mean in order to eliminate differences in the standard error of the mean of α due to the severalfold differences in the α values themselves. This measure of variability for the determination of α using cells and QSC beads is shown in A. In a single measurement, the standard error of the mean was calculated from about 30 cells or QSC beads. The error bars represent the standard deviation of the normalized standard errors. The α values along with their standard deviations are plotted in parts B–D.

calculated with cells (Figure 1A). The same tendencies were observed when SKBR-3 cells and QSC beads were labeled with AlexaFluor488-Mab528 and AlexaFluor546-Mab528, or when SKBR-3 cells and QSC beads were labeled with AlexaFluor488-trastuzumab and AlexaFluor546-trastuzumab. The consistently better reproducibility of α calculation using QSC beads was due to the lower variability of the intensity of beads compared to cells (Figure S3). We can conclude that the precision of the calculation of α using QSC beads is superior to when cells are used.

4.2 | Further improvement of the precision of parameter α by eliminating the need for two samples in measurements of homoassociation

Although the application of QSC beads clearly improves the reproducibility of the calculation of α, the results outlined in the previous section still require the comparison of the intensities of two samples. According to the principles outlined in the Theory section, in particular Equation (15), α can also be determined using a single sample. We expected a significant improvement in reproducibility since this approach eliminates the requirement for two samples altogether, and instead only involves intensity ratios of a single sample that can be determined with much better precision. The novel approach establishes a relationship between the donor (I_D) and acceptor (I_A) intensities, which requires an antibody mixture whose R' parameter has previously been determined. R' characterizes the fraction of binding sites occupied by the donor and also takes the degrees of labeling into consideration (Equation (12)). The fraction of binding sites occupied by one of the antibodies in an antibody mixture is constant for individual cells or beads if the donor-tagged and acceptor-tagged antibodies compete with each other for the same binding sites, which is most conveniently established in measurements of homoassociation, that is, when the donor- and acceptor-tagged antibodies are against the same epitope.

We determined parameter R' for a trastuzumab antibody mixture using SKBR-3 cells and QSC beads (Figure 2A), and for a Mab528 mixture using SKBR-3 and A431 cells as well as QSC beads (Figure 2B). R' for the trastuzumab mixture was not determined on A431 cells because they do not express ErbB2, the epitope of trastuzumab. The experiments were carried out with three antibody mixtures in which the donor-tagged and the acceptor-tagged antibodies were mixed at a 1:2, 1:1 and 2:1 ratio. The expected values of R' for these antibody mixtures, assuming equal affinities of donor- and acceptor-tagged antibodies to their binding sites and taking the degrees of labeling into consideration are 0.5, 1.1 and 2.2, respectively, for Mab528, and 0.4, 0.8 and 1.6, respectively, for trastuzumab. R' values of a certain antibody mixture determined with different cells or the QSC beads were remarkably similar, and they changed as expected upon changing the molar fraction of the donor-tagged antibody. Although, the

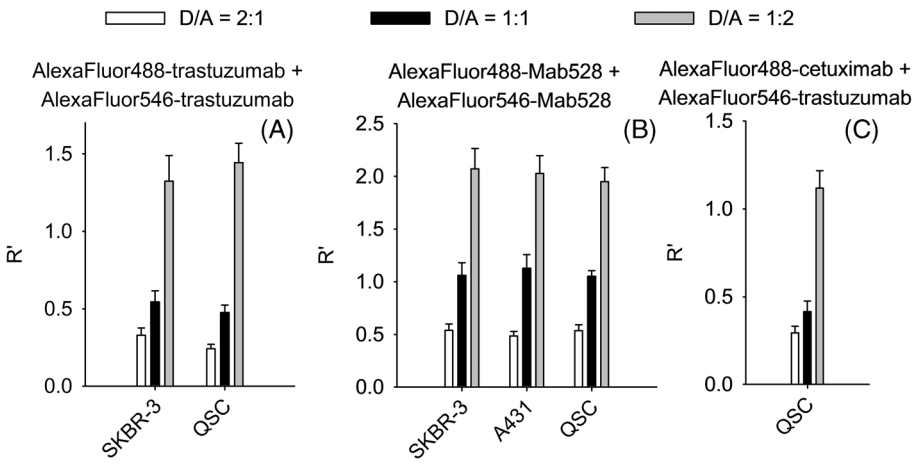

FIGURE 2 Determination of *R*'. Cells (SKBR-3, A431) or QSC beads were labeled with a mixture of antibodies in which the donor-tagged and acceptor-tagged IgGs were present in a molar ratio of 2:1, 1:1 and 1:2. Three different antibody mixtures were used in the experiment for the measurement of ErbB2 homoassociation (AlexaFluor488-trastuzumab + AlexaFluor546-trastuzumab), ErbB1 homoassociation (AlexaFluor488-Mab528 + AlexaFluor546-Mab528) and for determining the heterodimerization of EGFR and ErbB2 (AlexaFluor488-cetuximab + AlexaFluor546-trastuzumab). *R*' determined according to Equation (14) and the corresponding standard deviation of five independent measurements are plotted in the graphs.

determined *R*' values were close to the expected values for Mab528 (Figure 2B), they differed significantly for trastuzumab (Figure 2A). While the affinity of Mab528 was shown to be relatively insensitive to fluorescence labeling, trastuzumab's dissociation constant strongly deteriorates after fluorescence labeling in a fluorophore-dependent manner [24]. Therefore, the ratio of donor- and acceptor-tagged trastuzumab in the bound fraction is not equal to their ratio in the stock, providing an explanation for the aforementioned deviations of *R*' from the expected value. Although the equation for calculating *R*', Equation (14), does contain instrument-dependent parameters such as the overspill factors and α, *R*' must be instrument independent since it is a function of the ratio of binding sites occupied by the donor-tagged antibody and the degrees of labeling of the donor-conjugated and acceptor-conjugated antibodies, that is, properties of the antibody mixture only, as defined by Equations (5) and (12). Therefore, once it is determined for an antibody mixture in flow cytometry (where the large number of measured cells ensures statistical robustness), it can be used in microscopic measurements with the same antibody mixture.

Using these *R*' values we carried out confocal microscopic experiments in which cells or QSC beads were labeled with the same antibody mixtures, and α was determined according to Equation (15). The pipeline of the evaluation is shown in Supplementary Figure S1. Mean membrane/edge intensities of all cells/QSC beads corresponding to a certain condition were saved in a database, and bootstrapping was used for establishing the standard error of the mean (Suppl. Figure S2). The results reveal that the novel method involving *R*' for the determination of α is superior to the conventional method, and provides a low standard error even at small sample sizes ($N < 10$; Figure 3A,C,E). Furthermore, application of the *R*' approach results in equally reproducible results independent of whether cells or QSC beads are used. Bootstrapping confirmed that the conventional method involving two QSC bead samples for the determination of α provides better precision compared to the application of cells. Although the standard error of the mean of α determined using the *R*' approach is superior to those determined by the conventional approach, both methods provide mean values of α that are in accordance with each other (Figure 3B,D,F), confirming the accuracy of the *R*' approach. We can conclude that application of a single sample is a reliable approach for determining α even from few cells.

4.3 | Application of the novel method based on R' for heteroassociation measurements

In previous sections, both the conventional and the *R*'-based determination of α were applied to donor- and acceptor-conjugated versions of the same antibody. If parameter α is to be measured for a donor-acceptor pair in which the donor and the acceptor are conjugated to different kinds of antibodies, for example, in measurements of heteroassociation, only the QSC bead-based approach can be used since QSC beads bind a certain number of antibodies through their Fc region independent of their idiotype. Consequently, an equal number of the donor- and acceptor-tagged antibodies bind to the donor-labeled and the acceptor-labeled beads in the conventional approach, and they compete for the same binding sites, a feature required by the *R*'-based approach. We used this method to determine α for AlexaFluor488-cetuximab and AlexaFluor546-trastuzumab, humanized monoclonal antibodies against EGFR and ErbB2, respectively. We prepared three different mixtures of the donor- and acceptor-tagged antibodies and determined their *R*' parameter (Figure 2C). The deviation of the determined *R*' values from the expected values may be linked to differences in the affinities of the two antibodies to the anti-Fc coating of QSC beads. Using the *R*' values determined by flow

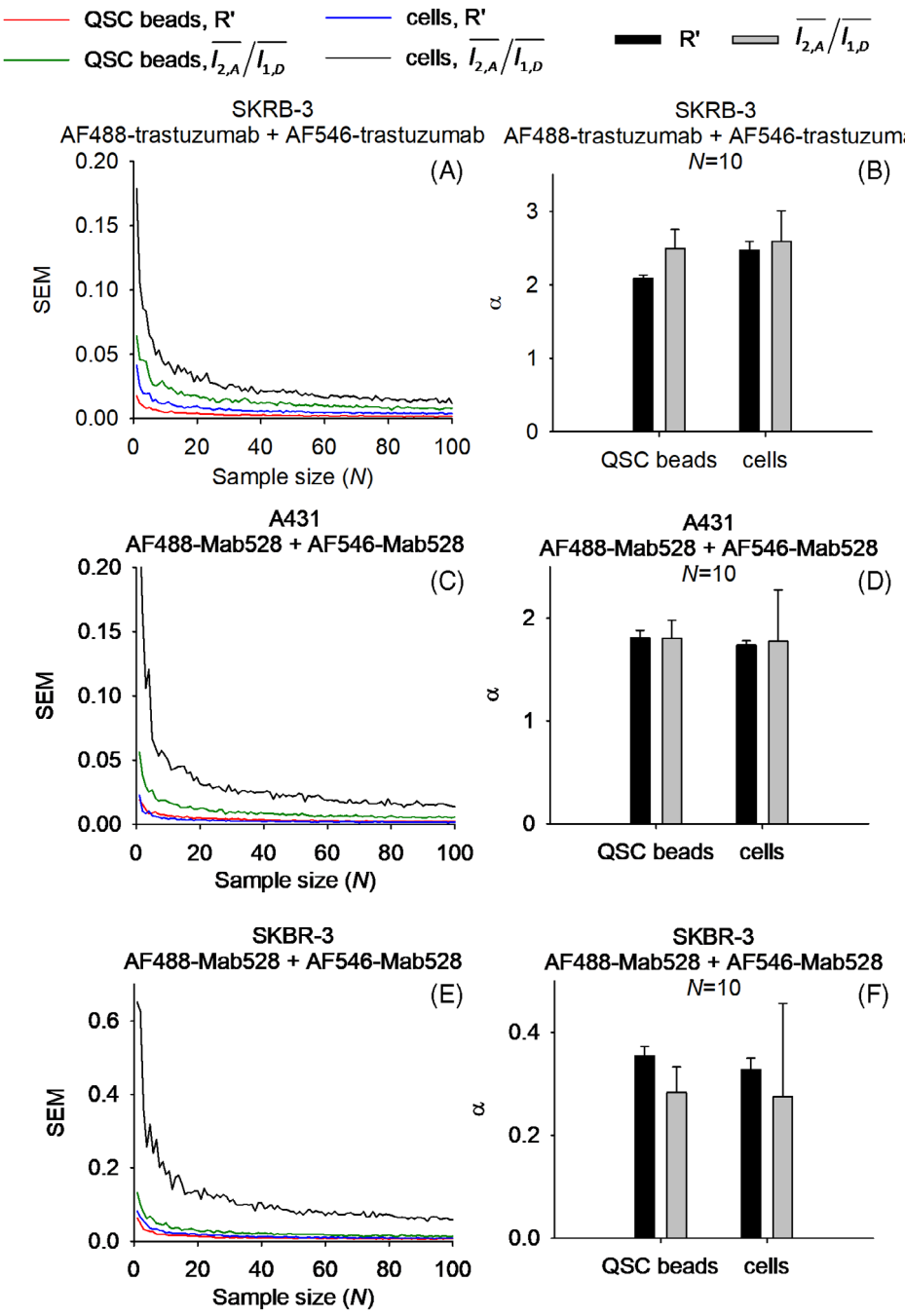

FIGURE 3 Reproducibility of determining α using the method involving *R'* compared to the conventional approach. SKBR-3 cells were labeled with an approximately 1:1 mixture of AlexaFluor488-conjugated and AlexaFluor546-conjugated trastuzumab (panels A–B; AlexaFluor is abbreviated AF in the figure). SKRB-3 or A431 cells were labeled with an approximately 1:1 mixture of AlexaFluor488-tagged and AlexaFluor546-tagged Mab528 (panels C–F). QSC beads were also labeled by the same mixtures of antibodies. The *R'* values of the antibody mixtures were determined previously by flow cytometry (Figure 2A,B). The donor-acceptor double-labeled cells and QSC beads were imaged by confocal microscopy, and the intensities of individual cells/beads measured in the donor, FRET and acceptor channels were determined. Random samples of size *N* were taken with replacement from these intensities (described in the "Statistical analysis" section in Materials and Methods), and α was calculated according to Equation (15). The procedure was repeated 100-times, and the standard error of the mean of α is plotted as a function of the sample size (red and blue curves in panels A, C and E). α was also calculated according to the conventional method with the same antibody pairs using cells and QSC beads, but two samples were generated in this approach. One of them was labeled by the AlexaFluor488-conjugated antibody, while the other one was only labeled by the AlexaFluor546-conjugated antibody. The samples were imaged and the intensities of individual cells were stored. Random samples of size *N* were independently taken from the donor-only and acceptor-only dataset, and α was calculated according to Equation (2). Repeating the procedure 100-times permitted the determination of the standard error of the mean, which is plotted as a function of the sample size (blue and black curves in panels A, C and E). The principle of the resampling approach is summarized in Supplementary Figure S2. The bar graphs on the right (panels B, D and F) show the mean value of α for a sample size of 10 along with the standard deviation determined according to the conventional method ($\overline{I_{2,A}}/\overline{I_{1,D}}$) and the *R'*-based approach. [Color figure can be viewed at wileyonlinelibrary.com]

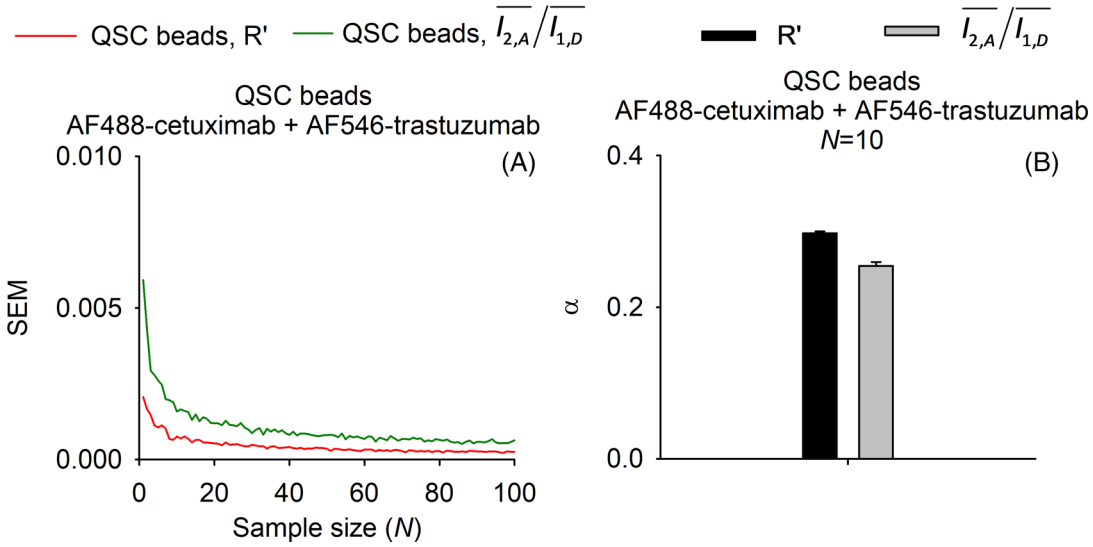

FIGURE 4 Determination of α for antibodies against different epitopes. Anti-human QSC beads were labeled with a mixture of AlexaFluor488-cetuximab and AlexaFluor546-trastuzumab and subsequently imaged by confocal microscopy. The *R'* value of the antibody mixture had been previously determined by flow cytometry (Figure 2C). The standard error of the mean of the approach involving *R'* and the conventional approach was estimated by the resampling approach described in the legend to Figure 3. The standard error of the mean is plotted as a function of the sample size (A). The bar graph on the right displays the mean value of α for a sample size of 10 along with the standard deviation. [Color figure can be viewed at wileyonlinelibrary.com]

cytometry, the same antibody mixtures were used for labeling QSC beads, and α was determined using the *R'*-based approach as in previous sections. Furthermore, α was also determined using the conventional approach using two samples of QSC beads, with one of them labeled with AlexaFluor488-cetuximab and the other one with AlexaFluor546-trastuzumab. The α values determined by the two approaches were in close agreement with each other, but reproducibility of the *R'*-based method was better (Figure 4).

5 | DISCUSSION

The intensity-based FRET measurement is an easily realizable approach for analyzing protein associations in living cells. Its unique advantage is its solid foundation on physical principles offering device independence in cross-platform implementations of the technique. Robustness of parameter α, a calibration factor relating the extent of donor quenching to the consequent sensitized emission of the acceptor, is pivotal for fulfilling the aforementioned potential. From among all the correction and calibration factors as well as the FRET efficiency, this is the only parameter in antibody-based FRET measurements that involves intensities determined from different samples. This circumstance deteriorates the reproducibility of parameter α if few cells are measured due to the low precision of mean intensities in such cases. The manuscript describes two improvements in determining α by (i) applying QSC microbeads with a precise number of binding sites; and (ii) by eliminating the requirement for two samples by using a mixture of donor-tagged and acceptor-tagged antibodies. The replacement of cells with QSC beads results in substantial improvement in the reproducibility of α, which is more pronounced when the cellular expression level of an antigen is low (e.g., Mab528 binding to SKBR-3 cells, Figures 1A and 3E). Elimination of the comparison of intensities of different samples in the *R'*-based approach leads to further reduction in the measurement error of α (Figure 3A,C,E, Figure 4A). The application of QSC beads has the additional advantage of being applicable to determining α either with the conventional or the *R'*-based approach for heteroassociation measurements, that is, for antibodies binding to different epitopes (Figure 4). Since this feature depends on both the donor- and the acceptor-conjugated antibodies binding to the QSC beads, this approach can only be used for antibody pairs in which both of the antibodies are either of human or mouse origin (since QSC beads are coated with either anti-human or anti-mouse Fc-specific antibodies). This flexibility is an important benefit of the new approach since α could only be determined previously for a donor-acceptor pair if the donor was conjugated to the same kind of antibody as the acceptor [10, 13]. It was assumed that α determined in this way can be used for calibrating FRET measurements between other antibodies since α only depends on the instrument and the dyes (Equation (1)). However, this supposition was proved wrong by revealing that α is antibody-dependent (Fig. 1B,C,D) since it is determined by the fluorescence quantum efficiencies, which were shown to be influenced by what kind of antibody the dye in conjugated to [24].

Another complication arises in the experimental determination of α as a result of the difference in the degree of labeling of the bound and unbound fractions of antibodies, and the consequent differences in the quantum efficiencies [24]. Therefore, α for cellular FRET measurements has to be determined with cell-bound antibodies, and not

with stock solutions. The application of QSC beads for the determination of α for cellular FRET measurements is a reasonable compromise since the binding affinity of fluorescent antibodies to their epitope deteriorates similarly to how their binding to Fc-receptors, present on the surface of QSC beads, is affected (our unpublished observations). An inherent limitation of Equation (2), used for the experimental determination of α, is the correction of intensities with the degrees of labeling usually determined by spectrophotometry. Since (i) photometry is incapable of determining concentrations below the micromolar range and (ii) other elaborate techniques for the determination of the degree of labeling are overly complicated for everyday use [30–32], these measurements are carried out with stock solutions by spectrophotometry, and cellular intensities are corrected with the degrees of labeling of the stock. Since the degree of labeling of the stock differs from that of the bound fraction [24], this circumstance introduces a systematic error into the calculations. As α, determined using Equation (2), is used in the determination of R' according to Equation (14), the R'-based approach is not devoid of this limitation either. However, the superb reproducibility of α provided by the R'-based method and the device-independence of the aforementioned misestimation result in significantly enhanced inter-laboratory correspondence.

R' depends on the fraction of epitopes occupied by the donor-conjugated antibody and the degrees of labeling of the antibodies according to Equation (12). Although its value could be calculated for a given mixture of donor-tagged and acceptor-tagged antibodies, we observed deviations from these expected values for certain antibodies (Figure 2). These observations clearly show that R' has to be determined experimentally, but also call for an explanation for the deviations. The unequal affinities of the donor- and acceptor-conjugated antibodies, inaccuracies in the determination of the number of dyes per antibody, the difference between the degrees of labeling of the bound fraction and that of the stock, and inaccurate pipetting can all contribute to these differences.

In conclusion, the application of beads with a precise number of antibody-binding sites and the R'-based approach lead to significant improvements in the reproducibility of determination of α. Since the Excel sheet available as Supplementary Material makes the calculation easy, we expect that the proposed methods will contribute to the robustness of intensity-based FRET measurements with antibodies.

AUTHOR CONTRIBUTIONS

Ágnes Batta: Investigation, Formal analysis, Writing - Original Draft, Visualization. **Tímea Hajdu**: Investigation, Formal analysis, Writing - Review & Editing. **Peter Nagy**: Conceptualization, Software, Writing - Original Draft, Writing - Review & Editing, Visualization, Supervision, Funding acquisition.

ACKNOWLEDGMENTS

This work was funded by the National Research, Development and Innovation Office, Hungary (ANN133421, K138075) and by the Faculty of Medicine, University of Debrecen.

CONFLICT OF INTEREST STATEMENT

The authors have no competing interests to declare.

DATA AVAILABILITY STATEMENT

Sample data supporting the findings of this study is available at flowrepository.org (https://flowrepository.org/id/FR-FCM-Z5QM). The full dataset is available from the corresponding author upon reasonable request.

REFERENCES

1. Szöllősi J, Damjanovich S, Mátyus L. Application of fluorescence resonance energy transfer in the clinical laboratory: routine and research. Cytometry. 1998;34:159–79.
2. Schneckenburger H. Förster resonance energy transfer-what can we learn and how can we use it? Methods Appl Fluoresc. 2019;8:013001.
3. Hetey S, Boros-Oláh B, Kuik-Rózsa T, Li Q, Karányi Z, Szabó Z, et al. Biophysical characterization of histone H3.3 K27M point mutation. Biochem Biophys Res Commun. 2017;490:868–75.
4. Perrin F. La fluorescence des solutions. AnnPhys(Paris). 1929;12:169–275.
5. Förster T. Energiewanderung und Fluoreszenz. Naturwissenschaften. 1946;33:166–75.
6. Szabó A, Szendi-Szatmári T, Szöllősi J, Nagy P. Quo vadis FRET? Förster's method in the era of superresolution. Methods Appl Fluoresc. 2020;8:032003.
7. Jares-Erijman EA, Jovin TM. FRET imaging. Nat Biotechnol. 2003;21:1387–95.
8. Zeug A, Woehler A, Neher E, Ponimaskin EG. Quantitative intensity-based FRET approaches--a comparative snapshot. Biophys J. 2012;103:1821–7.
9. Hoppe A, Christensen K, Swanson JA. Fluorescence resonance energy transfer-based stoichiometry in living cells. Biophys J. 2002;83:3652–64.
10. Trón L, Szöllősi J, Damjanovich S, Helliwell SH, Arndt-Jovin DJ, Jovin TM. Flow cytometric measurement of fluorescence resonance energy transfer on cell surfaces. Quantitative evaluation of the transfer efficiency on a cell-by-cell basis. Biophys J. 1984;45:939–46.
11. Szendi-Szatmári T, Szabó A, Szöllősi J, Nagy P. Reducing the detrimental effects of saturation phenomena in FRET microscopy. Anal Chem. 2019;91:6378–82.
12. Szöllősi J, Mátyus L, Trón L, Balázs M, Ember I, Fulwyler MJ, et al. Flow cytometric measurements of fluorescence energy transfer using single laser excitation. Cytometry. 1987;8:120–8.
13. Szöllősi J, Trón L, Damjanovich S, Helliwell SH, Arndt-Jovin D, Jovin TM. Fluorescence energy transfer measurements on cell surfaces: a critical comparison of steady-state fluorimetric and flow cytometric methods. Cytometry. 1984;5:210–6.
14. Nagy P, Vámosi G, Bodnár A, Lockett SJ, Szöllősi J. Intensity-based energy transfer measurements in digital imaging microscopy. Eur Biophys J. 1998;27:377–89.
15. Szabó Á, Nagy P. I am the alpha and the …gamma, and the G. Calibration of intensity-based FRET measurements. Cytometry A. 2021;99:369–71.
16. Grabolle M, Spieles M, Lesnyak V, Gaponik N, Eychmüller A, Resch-Genger U. Determination of the fluorescence quantum yield of quantum dots: suitable procedures and achievable uncertainties. Anal Chem. 2009;81:6285–94.
17. Wurth C, Grabolle M, Pauli J, Spieles M, Resch-Genger U. Relative and absolute determination of fluorescence quantum yields of transparent samples. Nat Protoc. 2013;8:1535–50.

18. Nagy P, Bene L, Hyun WC, Vereb G, Braun M, Antz C, et al. Novel calibration method for flow cytometric fluorescence resonance energy transfer measurements between visible fluorescent proteins. Cytometry A. 2005;67:86–96.
19. Chen H, Puhl HL 3rd, Koushik SV, Vogel SS, Ikeda SR. Measurement of FRET efficiency and ratio of donor to acceptor concentration in living cells. Biophys J. 2006;91:L39–41.
20. Hohlbein J, Craggs TD, Cordes T. Alternating-laser excitation: single-molecule FRET and beyond. Chem Soc Rev. 2014;43:1156–71.
21. Vámosi G, Baudendistel N, von der Lieth CW, Szalóki N, Mocsár G, Muller G, et al. Conformation of the c-Fos/c-Jun complex in vivo: a combined FRET, FCCS, and MD-modeling study. Biophys J. 2008;94:2859–68.
22. Szalóki N, Doan-Xuan QM, Szöllősi J, Tóth K, Vámosi G, Bacsó Z. High throughput FRET analysis of protein-protein interactions by slide-based imaging laser scanning cytometry. Cytometry A. 2013;83:818–29.
23. Menaesse A, Sumetsky D, Emanuely N, Stein JL, Gates EM, Hoffman BD, et al. Simplified instrument calibration for wide-field fluorescence resonance energy transfer (FRET) measured by the sensitized emission method. Cytometry A. 2021;99:407–16.
24. Szabó A, Szendi-Szatmári T, Ujlaky-Nagy L, Rádi I, Vereb G, Szöllősi J, et al. The effect of fluorophore conjugation on antibody affinity and the photophysical properties of dyes. Biophys J. 2018;114:688–700.
25. Zal T, Gascoigne NR. Photobleaching-corrected FRET efficiency imaging of live cells. Biophys J. 2004;86:3923–39.
26. Bene L, Bagdány M, Ungvári T, Damjanovich L. Information theoretic FRET calibration on the cell surface. J Photochem Photobiol A Chem. 2021;409:113144.
27. Bene L, Ungvári T, Fedor R, Sasi Szabó L, Damjanovich L. Intensity correlation-based calibration of FRET. Biophys J. 2013;105:2024–35.
28. Nagy P, Szabó A, Váradi T, Kovács T, Batta G, Szöllősi J. rFRET: a comprehensive, Matlab-based program for analyzing intensity-based ratiometric microscopic FRET experiments. Cytometry A. 2016;89:376–84.
29. Sebestyén Z, Nagy P, Horváth G, Vámosi G, Debets R, Gratama JW, et al. Long wavelength fluorophores and cell-by-cell correction for autofluorescence significantly improves the accuracy of flow cytometric energy transfer measurements on a dual-laser benchtop flow cytometer. Cytometry. 2002;48:124–35.
30. Delon A, Wang I, Lambert E, Mache S, Mache R, Derouard J, et al. Measuring, in solution, multiple-fluorophore labeling by combining fluorescence correlation spectroscopy and photobleaching. J Phys Chem B. 2010;114:2988–96.
31. Nayak CR, Rutenberg AD. Quantification of fluorophore copy number from intrinsic fluctuations during fluorescence photobleaching. Biophys J. 2011;101:2284–93.
32. Tsekouras K, Custer TC, Jashnsaz H, Walter NG, Presse S. A novel method to accurately locate and count large numbers of steps by photobleaching. Mol Biol Cell. 2016;27:3601–15.

SUPPORTING INFORMATION

Additional supporting information can be found online in the Supporting Information section at the end of this article.

How to cite this article: Batta Á, Hajdu T, Nagy P. Improved estimation of the ratio of detection efficiencies of excited acceptors and donors for FRET measurements. Cytometry. 2023;103(7):563–74. https://doi.org/10.1002/cyto.a.24728

SUPPLEMENTARY INFORMATION

Improved estimation of the ratio of detection efficiencies of excited acceptors and donors for FRET measurements

Ágnes Batta, Tímea Hajdu, Peter Nagy

Department of Biophysics and Cell Biology, Faculty of Medicine, University of Debrecen, Debrecen, Hungary

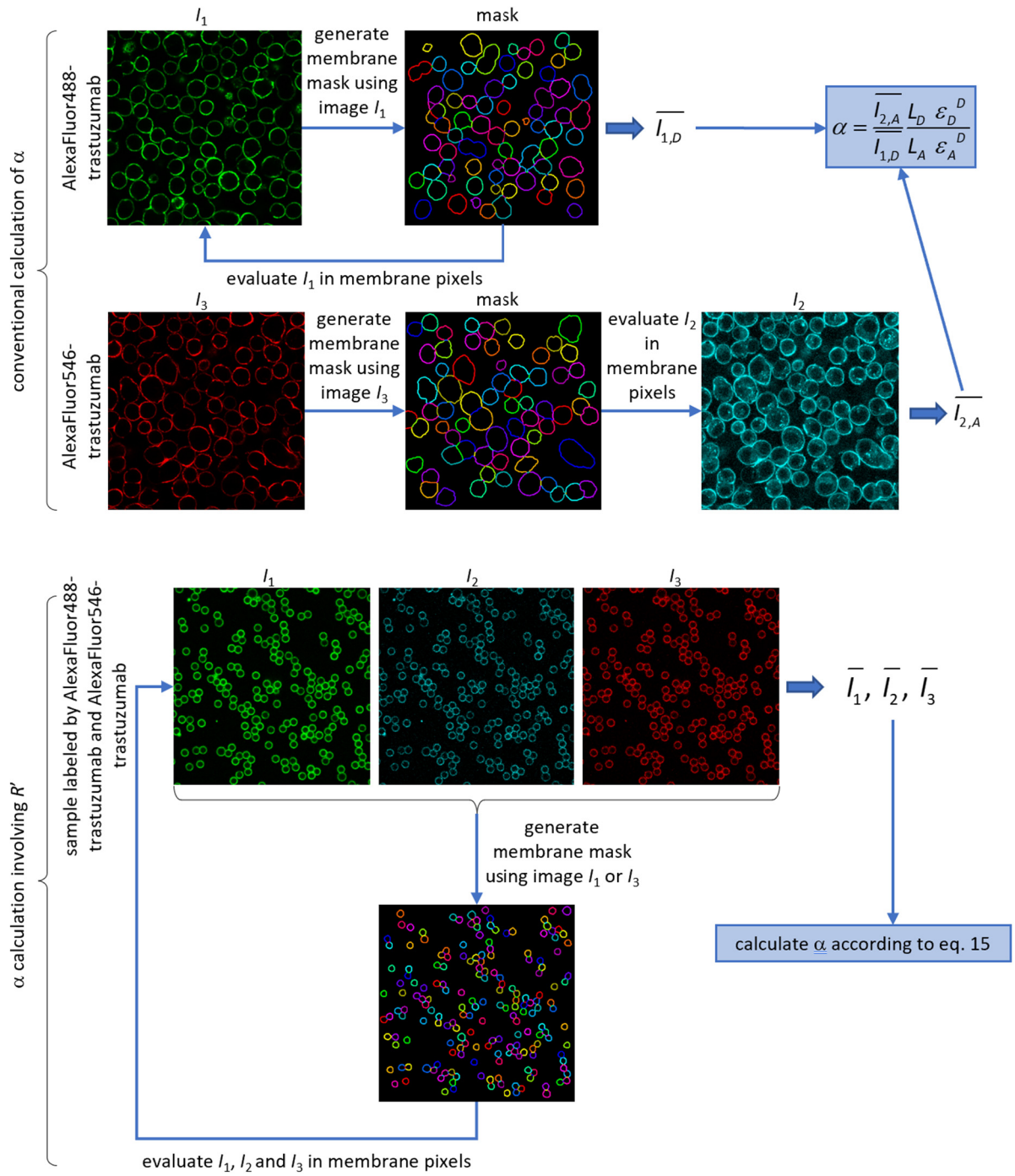

Supplementary Figure S1. Outline of calculation of α using confocal microscopic images. Conventional determination of α involves measuring two samples labeled by a donor-conjugated and an acceptor-conjugated version of the same antibody. The donor-only labeled sample is measured in the donor channel (I_1) followed by determining the mean intensity in this channel ($\overline{I_{1,D}}$) in pixels corresponding to the membrane mask that was determined using this same image. The sample labeled by the acceptor only is measured in the FRET (I_2) and acceptor (I_3) channels, and a membrane mask is determined using the brighter image (I_3). The

mean intensity in the FRET channel ($\overline{I_{2,A}}$) is determined in membrane pixels. The mean intensities are substituted into the equation $\alpha = \overline{I_{2,A}} / \overline{I_{1,D}} \left(L_D \ \varepsilon_D^{\ D} \right) / \left(L_A \ \varepsilon_A^{\ D} \right)$ providing α. For calculating α using *R*'-based approach, a sample is labeled with a mixture of donor-conjugated and acceptor-conjugated antibodies whose *R*' value was previously determined using flow cytometry. The labeled targets can be cells or QSC beads (QSC beads were used in the figure). A membrane mask is generated from the brightest image (I_1 or I_3) and intensities in all three channels are evaluated in the edge pixels. The mean I_1, I_2 and I_3 intensities are substituted into equation 15 of the main text providing α. The membrane masks in both approaches are determined by manually-seeded watershed segmentation. The intensity in the whole membrane of each individual cell is determined. Membrane segments shared by two cells, i.e., those membranes that separate two neighboring cells (labeled by different colors in the membrane masks) are treated differently from those membranes that belong to a single cell only. The intensity of shared membrane segments is divided by the number of cells sharing that membrane (usually two) when calculating the total intensity of a single cell.

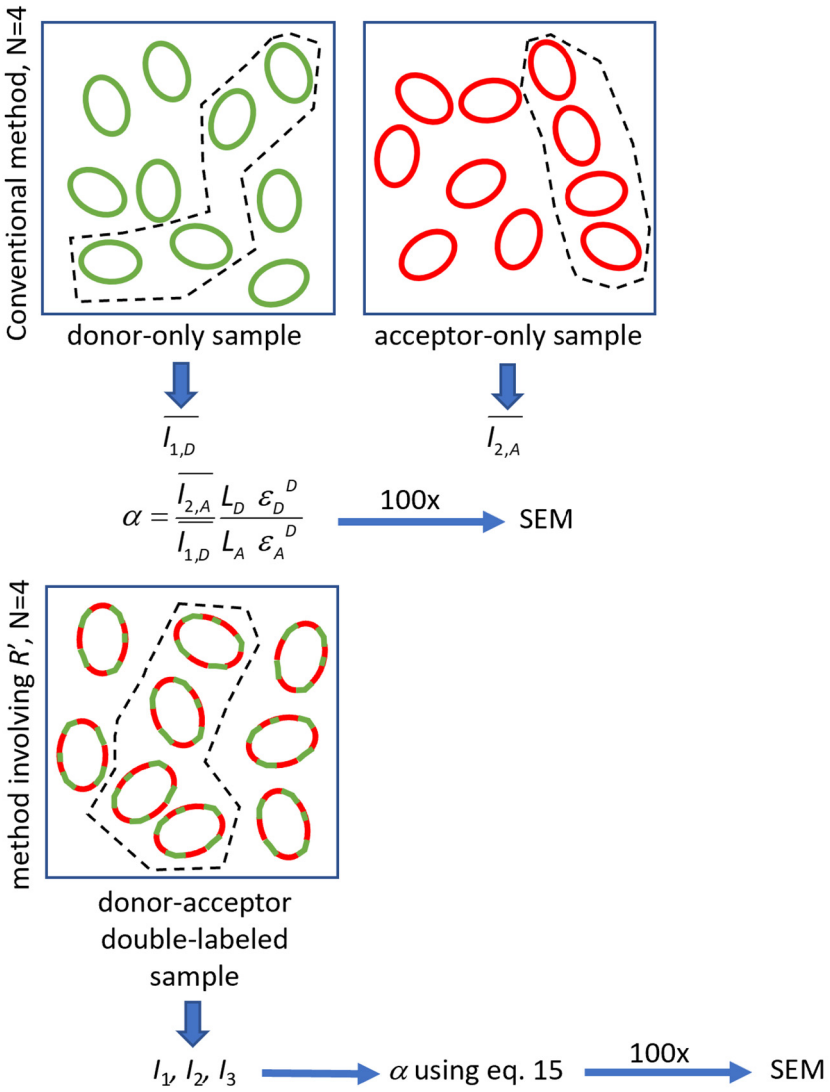

Supplementary Figure S2. Determination of the reproducibility of calculating α. For calculating α according to the conventional method, two samples labeled by a donor-conjugated and an acceptor-conjugated version of the same antibody were used. Intensities in membrane pixels were evaluated, and a certain number (*N*=4 in the figure) of cells were randomly chosen with replacement (as described in the "Statistical analysis" section of Materials and Methods) from both the donor-labeled and the acceptor-labeled samples, and their mean intensities were determined ($\overline{I_{2,A}}$, $\overline{I_{1,D}}$). The mean values were substituted into the equation shown in the figure and the procedure was repeated 100-times providing the standard error of the mean of α for a certain sample size (*N*=4 in the figure). For calculating α using the *R*'-based method, a sample labeled by both donor-tagged and acceptor-tagged antibodies was measured, and intensities were evaluated in membrane pixels. A certain number of cells were randomly chosen with replacement, and their mean intensities in the donor, FRET and acceptor channels were determined (I_1, I_2, I_3). Substituting these values into equation 15 of the main text provided α. The procedure was repeated 100-times yielding the standard error of the mean.

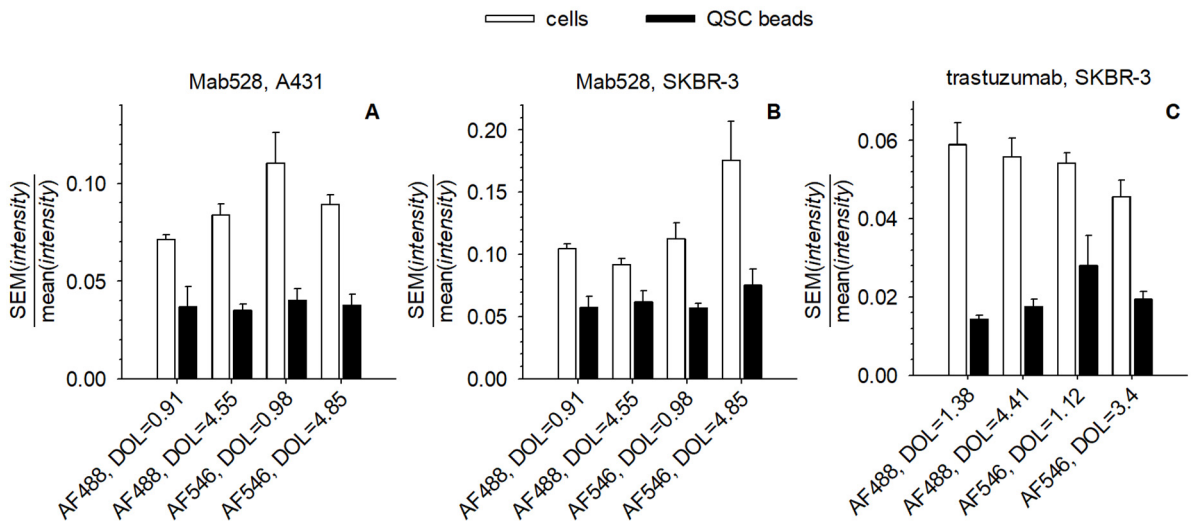

Supplementary Figure S3. Reproducibility of intensity measurements using cells and QSC beads. Cells or beads were labeled with either donor- or acceptor-conjugated antibodies followed by their measurement by confocal microscopy. The antibodies and their degrees of labeling (DOL) are labeled on the horizontal axes (AF488 – AlexaFluor488, AF546 – AlexaFluor546). The standard error of the mean of five independent measurements normalized by the mean is plotted in the figures. The error bars show the standard deviation of the standard error.

Supplementary Table 1. Workflow of determining α according to the conventional and *R*'-based methods.

Conventional method	*R*'-based method
• Label QSC beads with donor-tagged antibodies, and another sample of the same population (same number of binding sites) of QSC beads with acceptor-conjugated antibodies. Use anti-mouse and anti-human beads for antibodies of mouse and human origin, respectively.	• Label QSC beads with a mixture of donor-tagged and acceptor tagged antibodies. Label another sample of the same bead population (same number of binding sites) with the donor-conjugated antibody, and another sample with the acceptor-conjugated antibody. Use anti-mouse and anti-human beads for antibodies of mouse and human origin, respectively.
• Measure the intensity of ~50 donor-tagged beads in the donor channel by microscopy, and the intensity of approximately 50 acceptor-conjugated microspheres in the FRET or acceptor channel.	• Measure the double-labeled sample by flow cytometry. Enter the mean intensities in the donor, FRET and acceptor channels of the double-labeled sample into cells B4-D4 of the sheet "R' from flow cytometry" of the Excel file "alpha from R and QSC.xlsm".
• Determine a mask for edge pixels using e.g. marker-controlled (manually-seeded) watershed segmentation. Use the MATLAB program at http://peternagyweb.hu/Image-Analysis-with-Matlab.html#manual_watershed_section or the "Interactive Marker-controlled Watershed" plugin in FIJI (available as part of MorphoLibJ)	• Measure the single-labeled samples by flow cytometry. Enter their mean intensities into cells B2 and D3 of the same Excel sheet. Determine overspill parameters S1-S4 (cells B6-B9) using the donor-only and acceptor-only samples. Determine the molar absorption coefficients and the degrees of labeling, and enter them into the corresponding cells of the Excel sheet. Once all parameters are filled in, *R*' is displayed in cell B17.
• Determine the degree of labeling of the antibodies and the molar absorption coefficients of the donor and acceptor at the donor excitation wavelength. Enter these values into cells B5-B6 and F3-F4 of sheet "Conventional method" of the Excel file "alpha from R and QSC.xlsm".	• Measure the same three samples by confocal microscopy. Alternatively, a new sample series can be labeled as long as the same antibody mixture is used whose *R*' parameter has been determined by flow cytometry.
• Determine the mean intensities in the donor-labeled and in the acceptor-labeled samples in pixels corresponding to the mask, and calculate α according to equation 2 of the main text by entering these mean intensities into cells B2 and B3 (or B4) of the Excel sheet. If the intensity of the acceptor-conjugated sample was measured in the acceptor channel, overspill parameter S2 is to be determined as well.	• Determine spectral overspill parameters using the single-labeled samples, and enter them into cells B4-B7 of the Excel sheet "alpha from CLSM using R'". Determine the mean intensities of ~20 double-labeled QSC beads in the donor, FRET and acceptor channels, and enter them into cells B2-D2. Use only edge pixels determined as described in the left column for "Conventional method". • Enter the *R*' value of the antibody mixture (cell B8) that was determined by flow cytometry. • Determine and enter the molar absorption coefficients. These are not necessarily equal to the ones used in the previous sheet ("R' from flow cytometry") since the excitation wavelengths used in flow cytometry and microscopy may differ. • Once all values are entered, parameter α is displayed in cell B13.